

## Evolution of a Large Fermi Surface in the Kondo Lattice

Junya Otsuki,<sup>1</sup> Hiroaki Kusunose,<sup>2</sup> and Yoshio Kuramoto<sup>1</sup>

<sup>1</sup>*Department of Physics, Tohoku University, Sendai 980-8578, Japan*

<sup>2</sup>*Department of Physics, Ehime University, Matsuyama 790-8577, Japan*

(Received 31 July 2008; published 5 January 2009)

The single-particle spectrum of the Kondo lattice model is derived with the use of the continuous-time quantum Monte Carlo method, combined with the dynamical mean-field theory. Crossover behavior is traced quantitatively either to a heavy Fermi-liquid state or to a magnetically ordered state from the local-moment state at high temperatures. The momentum distribution in the low-temperature limit acquires a discontinuity at the location that involves the local-spin degrees of freedom. Even without the charge degrees of freedom for local electrons, the excitation spectra exhibit hybridized bands similar to those in the Anderson lattice. Temperature dependence in the zero-energy component of the self-energy is crucial in forming the Fermi-liquid state with the large Fermi surface.

DOI: 10.1103/PhysRevLett.102.017202

PACS numbers: 75.20.Hr, 71.27.+a, 71.10.-w

A long-standing problem in condensed matter physics is how to resolve the dichotomy between localized and itinerant characters of electrons in solids. For many metals with  $f$  electrons, and also some with  $d$  electrons, the strong Coulomb repulsion between localized electrons suppresses charge fluctuations at each site, leaving only a spin and/or an orbital degree of freedom. These localized degrees of freedom interact with conduction electrons, which are delocalized over the entire crystal. The itinerant and localized electrons affect each other and realize rich physical phenomena such as heavy electrons.

The simplest model to describe the situation is the Kondo lattice model (KLM) given by

$$H = \sum_{k\sigma} \epsilon_k c_{k\sigma}^\dagger c_{k\sigma} + J \sum_i \mathbf{S}_i \cdot \boldsymbol{\sigma}_i. \quad (1)$$

Here  $\mathbf{S}_i$  represents the localized spin of the valence electron at the  $i$  site, and  $\boldsymbol{\sigma}_i = \sum_{\sigma\sigma'} c_{i\sigma}^\dagger \boldsymbol{\sigma}_{\sigma\sigma'} c_{i\sigma'}$  is the spin operator of the itinerant conduction electron. The antiferromagnetic exchange interaction  $J > 0$  under realistic conditions is much smaller than the bandwidth, and each localized spin acts as a weak scatterer for the conduction electrons at high temperatures. As temperature decreases, interactions between the localized spins become significant, which are mediated by conduction electrons, and a magnetic long-range order may be realized. On the other hand, the localized spins also tend to be quenched by conduction electrons, which is called the Kondo effect. If the system remains paramagnetic, coherent quasiparticles may emerge by the collective Kondo effect. Although the overall picture [1] mentioned above is widely accepted, the rich crossover phenomena due to emergent quasiparticles remain highly nontrivial [2].

The KLM has no apparent counterpart of a noninteracting system, since the perturbation series with respect to  $J$  is essentially singular at  $J = 0$ . Accordingly, we have no clear starting point to study the nature of the paramagnetic

ground state in the KLM. On the other hand, an ordinary Fermi-liquid argument is applicable to the Anderson lattice, since the adiabatically continued noninteracting ground state is evident [3]. A clue for characterizing the KLM is Luttinger's theorem which relates the volume of the Fermi surface with the number of electrons [4]. A version of the proof [5] of this theorem states that the volume of the Fermi surface is the same as that in the Anderson lattice (the so-called "large Fermi surface") with unit occupation of each local state. The proof is valid provided that the ground state of the KLM is a Fermi liquid. However, it is not trivial whether this condition is satisfied. In fact, another possibility of a "small" Fermi surface has also been proposed [6–8] with inclusion of explicit coupling between local spins.

Because of the difficulty in including higher-order effects of  $J$ , the KLM has been studied either by variants of the mean-field theory [7,9,10] or in one-dimensional systems [11–13]. In the mean-field theory, the collective Kondo effect appears as a phase transition, and it is difficult to reproduce the Kondo crossover at finite temperatures. As a particular feature in one dimension, on the other hand, the low-energy excitations behave as in a Tomonaga-Luttinger liquid without discontinuity in the momentum distribution. Furthermore, a magnetic long-range order, which competes with the paramagnetic state, is strongly suppressed. Thus it is highly desirable to obtain reliable information in higher dimensions, especially the temperature-dependent evolution of the collective Kondo effect.

In this Letter, we report results which become exact in the limit of infinite dimensions. First, evolution of the Landau quasiparticles is traced quantitatively from the local-moment regime at high temperatures. Second, a magnetic phase diagram of the KLM is derived. The periodic lattice effect is dealt with by the dynamical mean-field theory (DMFT) [14]. To solve the effective impurity problem in the DMFT, we use the continuous-time quantum

Monte Carlo (CT-QMC) algorithm [15,16], adapted to the Kondo model [17]. Since no approximation such as discretization is involved in the CT-QMC algorithm, and since the simulation does not encounter the minus sign problem, the effective impurity problem can be solved with desired accuracy.

*Model and method.*—Let us start with the conduction-electron Green function in the KLM:

$$G_c(\mathbf{k}, i\epsilon_n) = [i\epsilon_n - \epsilon_{\mathbf{k}} + \mu - \Sigma_c(i\epsilon_n)]^{-1}, \quad (2)$$

where  $\epsilon_n = (2n + 1)\pi T$  is the fermionic Matsubara frequency. The self-energy  $\Sigma_c(i\epsilon_n)$  takes account of nonperturbative contributions from the localized spins, but the momentum dependence has been neglected according to the DMFT. The KLM is then mapped to the impurity Kondo model in the effective medium, which is characterized by the cavity Green function  $\mathcal{G}_c^0(i\epsilon_n)$ . The impurity self-energy  $\Sigma_c(i\epsilon_n)$  should be identical with that in Eq. (2) and is given in terms of the impurity  $t$  matrix  $t(i\epsilon_n)$  as  $\Sigma_c(i\epsilon_n)^{-1} = t(i\epsilon_n)^{-1} + \mathcal{G}_c^0(i\epsilon_n)$ . Here  $\mathcal{G}_c^0(i\epsilon_n)$  is determined from the local Green function  $\bar{G}_c(i\epsilon_n)$  of the lattice system via  $\mathcal{G}_c^0(i\epsilon_n)^{-1} = \bar{G}_c(i\epsilon_n)^{-1} + \Sigma_c(i\epsilon_n)$ .

We adopt a nearest-neighbor tight-binding model in the infinite-dimensional hypercubic lattice [18], which is characterized by the Gaussian density of states:  $\rho_c(\omega) = D^{-1}\sqrt{2/\pi}\exp(-2\omega^2/D^2)$ . We take  $D = 1$  as the unit of energy and fix the conduction-electron density per site as  $n_c = 0.9$  throughout this Letter. The latter choice favors antiferromagnetism by the nearly nesting condition. We use  $10^7$  QMC samples at most with 10–100 intervals. The DMFT self-consistent equations converge typically within 10 iterations.

*Phase diagram.*—We first show the  $J$ - $T$  phase diagram in Fig. 1. The antiferromagnetic transition temperature  $T_{AF}$  is determined by the divergence of the staggered magnetic susceptibility, which can be computed in terms of the Bethe-Salpeter equation with numerically derived local vertices [14,19]. Here we have neglected possible incom-

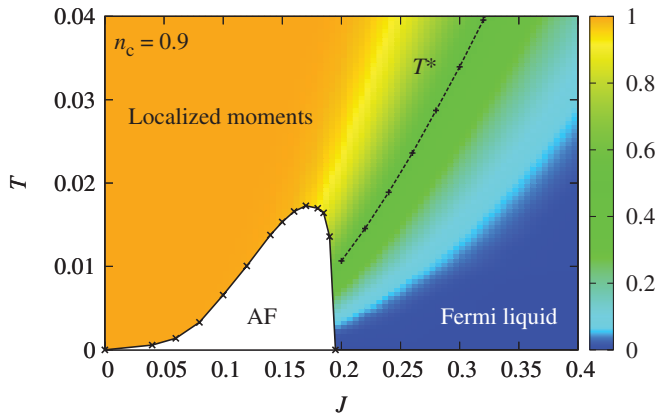


FIG. 1 (color). The phase diagram of the KLM at  $n_c = 0.9$ . The intensity map represents  $\xi$  defined by Eq. (6), and the coherent energy scale  $T^*$  is defined by  $\xi = 0.5$ .

mensurate order for simplicity, since our main interest in this Letter lies in the paramagnetic phase. The overall structure of the phase diagram is understood by competition between the Kondo effect and the RKKY interaction [1]. As  $J$  increases ( $T$  decreases) in the paramagnetic phase, the localized moments gradually disappear, and the Fermi-liquid behavior dominates below the coherent energy scale  $T^*$ . The intensity map in Fig. 1 represents the degree of itinerancy in terms of the parameter  $\xi$ , whose definition is given later in Eq. (6). We will show that the Fermi liquid is indeed realized for  $J > J_c \simeq 0.2$  at low temperatures. The crossover region in temperature becomes narrower near the quantum critical point,  $J_c$ .

*Single-particle spectra.*—In the DMFT,  $\mathbf{k}$  dependence of the Green function enters only through  $\epsilon_{\mathbf{k}}$ . Therefore  $G_c(\mathbf{k}, i\epsilon_n)$  is regarded as a function of  $\kappa = \epsilon_{\mathbf{k}}$  and is written as

$$G_c(\kappa, i\epsilon_n) = [i\epsilon_n - \kappa + \mu - \Sigma_c(i\epsilon_n)]^{-1}. \quad (3)$$

The single-particle excitation spectrum  $A(\kappa, \omega) = -\text{Im}G_c(\kappa, \omega + i0)/\pi$  is obtained by means of the Padé approximation [20]. The validity of the Padé approximation has been confirmed for the impurity Kondo-type models [17]. Our QMC data have accuracy high enough to obtain reliable real-frequency spectra.

Figure 2 shows the single-particle excitation spectra for a fixed value of  $J = 0.3$ . We define two energies  $\kappa_L$  and  $\kappa_S$  corresponding to the large and small Fermi surfaces, respectively. The upper panel shows  $A(\kappa, \omega)$  for  $T = 0.25$ . The spectrum exhibits a behavior of almost noninteracting electrons at high energies. However, the coupling with spin fluctuations gives rise to a pseudogap near the small Fermi surface  $\kappa_S$ .

The lower panel shows the spectrum at  $T = 0.0025$ , which is much lower than the impurity Kondo temperature defined by  $T_K = \sqrt{g}e^{-1/g} \sim 0.1$ , with  $g = 2J\rho_c(0)$ . The pseudogap looks like a true gap, and the coherent quasiparticles develop near the gap edges. This structure has a close resemblance to the hybridized band in the Anderson lattice. In particular, the width of the pseudogap is the order of the Kondo temperature  $T_K \sim 0.1$ . The quasiparticle intensity becomes sharper near the Fermi energy, and the quasiparticle band crosses the Fermi energy exactly at  $\kappa_L$ . Namely, the localized spins do contribute to the Fermi volume.

*Evolution of the Fermi liquid.*—Let us characterize the Green function near the Fermi surface. We expand the self-energy in powers of  $i\epsilon_n$  to obtain

$$G_c(\kappa, i\epsilon_n) \simeq \frac{z}{i\epsilon_n - z[\kappa - \mu + \Sigma_c(0)]}, \quad (4)$$

where the renormalization factor  $z$  is given by

$$z = \left(1 - \frac{\partial \text{Im}\Sigma_c(i\epsilon_n)}{\partial \epsilon_n} \Big|_{\epsilon_n \rightarrow +0}\right)^{-1}. \quad (5)$$

From the QMC data, we have confirmed numerically the

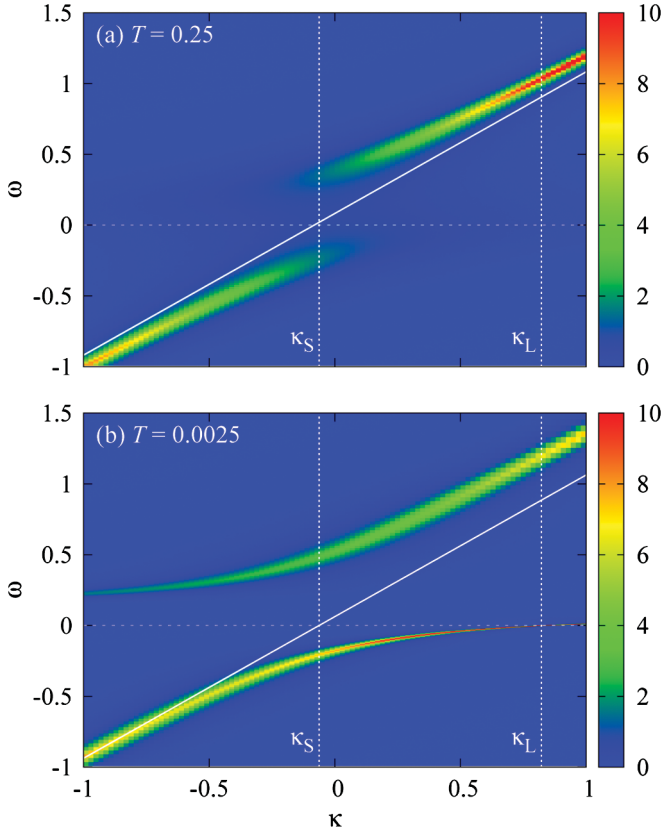


FIG. 2 (color). The single-particle excitation spectrum  $A(\kappa, \omega)$  for  $J = 0.3$  and  $n_c = 0.9$  at (a)  $T = 0.25$  and (b)  $T = 0.0025$ . The slanted line represents the noninteracting spectrum  $\omega = \kappa - \mu$  which is realized with  $J = 0$ .

Fermi-liquid conditions  $\partial \text{Re}\Sigma_c(i\epsilon_n)/\partial \epsilon_n \rightarrow 0$  and  $\text{Im}\Sigma_c(i\epsilon_n) \rightarrow 0$  in the limit  $\epsilon_n \rightarrow 0$ , which means  $T \rightarrow 0$ . As a result, we obtain  $z \simeq 0.084$  for  $J = 0.3$ . We extrapolate  $\text{Re}\Sigma_c(0)$  from the QMC data of  $\text{Re}\Sigma_c(i\epsilon_n)$  for small  $|n|$ , assuming a quadratic function centered at  $\epsilon_n = 0$ .

We now demonstrate the evolution of the Fermi-liquid state with the large Fermi surface as a function of temperature. The Fermi surface appears at such momentum that satisfies  $\epsilon_k = \mu - \Sigma_c(0)$ . Figure 3 shows temperature dependences of  $\mu - \text{Re}\Sigma_c(0)$  and  $\mu$  for  $J = 0.2, 0.3$ , and  $0.4$ . There are apparently two regimes in temperature. At high temperature, the self-energy correction is not important, and thermal excitations occur around  $\mu \sim \kappa_S$ . At low temperature, on the other hand,  $\mu - \text{Re}\Sigma_c(0)$  deviates significantly from  $\mu$  and gives rise to the large Fermi surface at  $\kappa_L$ . From this observation,  $\mu - \text{Re}\Sigma_c(0)$  turns out to be a good measure to characterize the crossover between the local-moment regime and the Fermi-liquid state. We introduce a dimensionless quantity

$$\xi = [\mu - \text{Re}\Sigma_c(0) - \kappa_L]/(\kappa_S - \kappa_L), \quad (6)$$

which ranges from 0 to 1 for  $T \ll D$ . The limit  $\xi = 0$  represents the Fermi-liquid state with the large Fermi surface, and the other limit  $\xi = 1$  represents almost non-interacting conduction electrons. We define the crossover

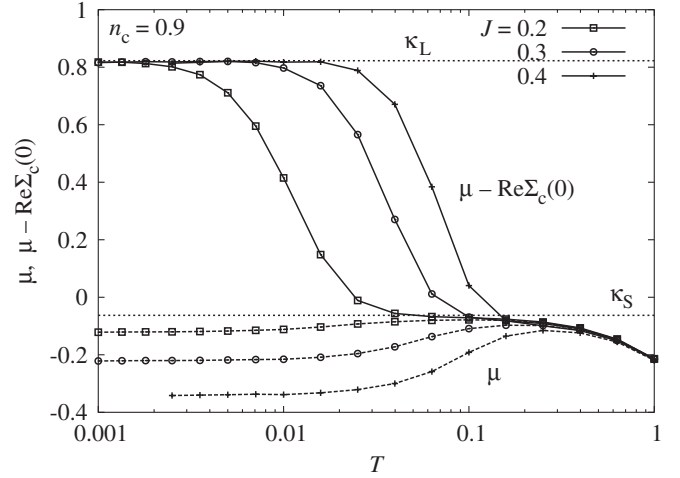


FIG. 3. Temperature dependences of the chemical potential  $\mu$  and its self-energy correction  $\mu - \text{Re}\Sigma_c(0)$  for  $n_c = 0.9$ .

temperature  $T^*$  by the condition  $\xi = 0.5$  as shown in Fig. 1. At  $J = 0.3$ , for example, we obtain  $T^* \simeq 0.035$ , which is smaller than  $T_K \sim 0.1$ .

For the one-dimensional KLM, the existence of two different energy scales has already been discussed in the literature [21]. The uniform charge susceptibility  $\chi_c(T)$ , for example, takes a maximum around  $T_K$  and decreases with decreasing temperature due to the development of the pseudogap. With a further decrease of temperature,  $\chi_c(T)$  turns to increase reflecting the contribution of coherent excitations, and it saturates to a finite value. For the infinite-dimensional KLM, our results of the uniform charge susceptibility, which will be reported elsewhere, show similar behavior with that in one dimension. The distinct energy scales without phase transitions are important to analyze experimental data properly.

We note the difference between the present description in Eq. (4) and the ordinary Fermi-liquid state in the Anderson lattice [3]. In the Anderson lattice, the localized electrons which are practically immobile at high temperatures eventually become itinerant. Thus, the major component of the quasiparticle is the localized electron. On the contrary, the local spins in the KLM remain absolutely immobile although the Fermi surface becomes large. At high temperatures, the conduction electrons interact incoherently with local-spin fluctuations. At low temperatures and energies, the conduction electrons manage to form coherent quasiparticles which accompany the polarization cloud of spin fluctuations. These quasiparticles exhibit the heavy-fermion behavior. In particular, the origin of the large linear specific heat is the entropy of the local spins as in the Anderson lattice. The spin entropy changes in the temperature scale of  $T_K$ .

*Momentum distribution.*—We now discuss the momentum distribution of conduction electrons:

$$\langle c_{k\sigma}^\dagger c_{k\sigma} \rangle = T \sum_n G_c(\kappa, i\epsilon_n) e^{i\epsilon_n 0^+} \equiv n_c(\kappa). \quad (7)$$

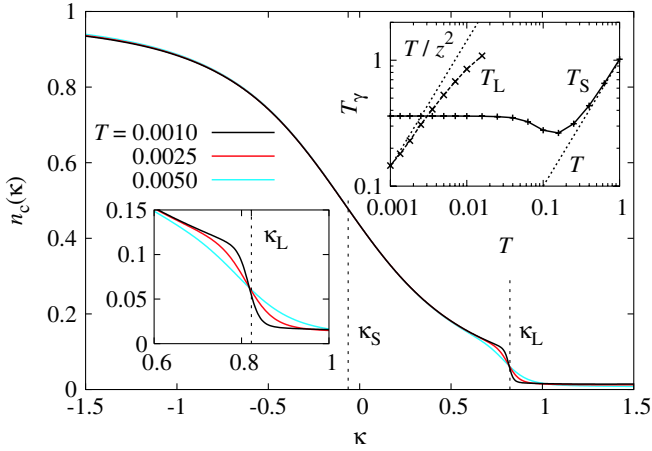


FIG. 4 (color online). Momentum distribution  $n_c(\kappa)$  for  $J = 0.3$  and  $n_c = 0.9$ . The vicinity of the large Fermi surface is enlarged in the left inset. The right inset shows the temperature dependences of the “width” of  $n_c(\kappa)$  at  $\kappa = \kappa_S$  and  $\kappa_L$ .

Figure 4 shows  $n_c(\kappa)$  in the Fermi-liquid state  $T \ll T^*$ . The gradient of  $n_c(\kappa)$  at  $\kappa = \kappa_L$  becomes steep with decreasing temperature, indicating the existence of discontinuity at  $T = 0$ . The magnitude of the discontinuity is consistent with  $z \simeq 0.084$  estimated from  $\sum_c(i\epsilon_n)$ . On the other hand,  $n_c(\kappa)$  at  $\kappa_S$  is almost independent of  $T$  in the Fermi-liquid state. For characterization of the momentum distribution at finite temperature, we introduce the energy scales ( $\gamma = L, S$ ):

$$T_\gamma = \frac{1}{4} \left( - \frac{\partial n_c(\kappa)}{\partial \kappa} \Big|_{\kappa=\kappa_\gamma} \right)^{-1} \quad (8)$$

at  $\kappa_L$  and  $\kappa_S$ . In the Fermi-liquid state with the approximate Green function [Eq. (4)],  $T_L$  should behave as  $T/z^2$ . The inset in Fig. 4 shows the temperature dependences of  $T_\gamma$ . The linear- $T$  dependence in  $T_L \simeq T/z^2$  at temperatures lower than  $T^*$  ( $\simeq 0.035$  for  $J = 0.3$ ) verifies the existence of the discontinuity at  $T = 0$  and ensures the validity of the quasiparticle expansion in Eq. (4). At temperatures higher than  $T_K$ , on the other hand,  $\kappa_L$  loses its importance. Instead, thermal excitations are populated around  $\mu \sim \kappa_S$  which develops according to  $T_S \simeq T$ .

We have thus established the Fermi-liquid state of the KLM in infinite dimensions. On the basis of Luttinger’s theorem, we may further develop a phenomenological Fermi-liquid theory in the vicinity of the large Fermi surface. Note that the Fermi-liquid state realized in the KLM has no explicit counterpart of a noninteracting system. This situation is identical to the local Fermi-liquid theory by Nozières in the single-impurity Kondo model [22], where the phase shift of conduction electrons is a key quantity. Following a similar strategy, an extension should be possible starting from the large Fermi surface in the three-dimensional KLM. Investigation of possible super-

conductivity is also a challenging issue in extending the present infinite-dimensional theory for the KLM.

In summary, we have demonstrated the temperature-dependent evolution of the Fermi-liquid state with the large Fermi surface. Our numerical results in the low-temperature limit confirm the premise for Luttinger’s theorem that relies on the Fermi-liquid character of low-energy excitations [5].

We acknowledge valuable discussions with N. Shibata and H. Yokoyama. One of the authors (J. O.) was supported by the Japan Society for the Promotion of Science for Young Scientists.

- [1] S. Doniach, *Physica* (Amsterdam) **91B+C**, 231 (1977).
- [2] For a review, see, for example, Y. Kuramoto and Y. Kitaoka, *Dynamics of Heavy Electrons* (Oxford University Press, New York, 2000).
- [3] For a review, see, for example, K. Yamada, *Electron Correlation in Metals* (Cambridge University Press, Cambridge, England, 2004).
- [4] J. M. Luttinger, *Phys. Rev.* **119**, 1153 (1960); **121**, 942 (1961).
- [5] M. Oshikawa, *Phys. Rev. Lett.* **84**, 3370 (2000).
- [6] P. Coleman and N. Andrei, *J. Phys. Condens. Matter* **1**, 4057 (1989).
- [7] S. Burdin, A. Georges, and D. R. Grempel, *Phys. Rev. B* **66**, 045111 (2002).
- [8] T. Senthil, S. Sachdev, and M. Vojta, *Phys. Rev. Lett.* **90**, 216403 (2003).
- [9] C. Lacroix and M. Cyrot, *Phys. Rev. B* **20**, 1969 (1979).
- [10] H. Shiba and P. Fazekas, *Prog. Theor. Phys. Suppl.* **101**, 403 (1990).
- [11] S. Moukouri and L. G. Caron, *Phys. Rev. B* **54**, 12212 (1996).
- [12] For a review, see H. Tsunetsugu, M. Sigrist, and K. Ueda, *Rev. Mod. Phys.* **69**, 809 (1997).
- [13] N. Shibata and K. Ueda, *J. Phys. Condens. Matter* **11**, R1 (1999).
- [14] For a review, see A. Georges, G. Kotliar, W. Krauth, and M. J. Rozenberg, *Rev. Mod. Phys.* **68**, 13 (1996).
- [15] A. N. Rubtsov, V. V. Savkin, and A. I. Lichtenstein, *Phys. Rev. B* **72**, 035122 (2005).
- [16] P. Werner, A. Comanac, L. de’Medici, M. Troyer, and A. J. Millis, *Phys. Rev. Lett.* **97**, 076405 (2006).
- [17] J. Otsuki, H. Kusunose, P. Werner, and Y. Kuramoto, *J. Phys. Soc. Jpn.* **76**, 114707 (2007).
- [18] E. Müller-Hartmann, *Z. Phys. B* **74**, 507 (1989).
- [19] For Kondo-type models, a calculation of the two-particle Green function is more involved. For details, see J. Otsuki, H. Kusunose, and Y. Kuramoto, *J. Phys. Soc. Jpn.* **78**, 014702 (2009).
- [20] H. J. Vidberg and J. W. Serene, *J. Low Temp. Phys.* **29**, 179 (1977).
- [21] N. Shibata and H. Tsunetsugu, *J. Phys. Soc. Jpn.* **68**, 744 (1999).
- [22] P. Nozières, *J. Low Temp. Phys.* **17**, 31 (1974).